Transition Effects on Slender Cone Pitch Damping

L. E. Ericsson*
Lockheed Missiles & Space Company Inc., Sunnyvale, California

A previously developed analytic theory for the effects of boundary-layer transition on slender cone pitch damping is amended to account for the fact that when the vehicle is perturbed from zero angle of attack, transition no longer occurs through Tollmien-Schlichting instability of the axial flow but through crossflow (inflexional) instability. This greatly improves the agreement between predicted and measured dynamic transition effects.

Nomenclature

c = reference length, $c = d_B$
D_N = nose drag, coefficient $C_{DN} = D_N/(\rho_\infty U_\infty^2/2)(\pi d_N^2/4)$
d = cone diameter
ℓ = body length
M = Mach number
M_p = pitching moment, coefficient $C_m = M_p/(\rho_\infty U_\infty^2/2)Sc$
N = normal force, coefficient $C_N = N/(\rho_\infty U_\infty^2/2)S$
p = static pressure, coefficient $C_p = (p-p_\infty)/(\rho_\infty U_\infty^2/2)$
q = rigid body pitch rate
R_ℓ = Reynolds number based on body length, $R_{\ell_\infty} = \ell U_\infty/\nu_\infty$
S = reference area, $S = \pi c^2/4$
t = time
Δt = time lag
U = axial velocity at $\alpha = 0$
x = axial body-fixed coordinate, distance from apex
α = angle of attack
$\tilde{\alpha}$ = generalized angle of attack, Eq. (2)
α_0 = trim angle of attack
Δ = difference or amplitude
δ = boundary-layer thickness
ϵ = crossflow inclination (Fig. 8)
θ = pitch perturbation
θ_c = cone half-angle
ν = kinematic viscosity of air
ξ = dimensionless axial coordinate, $\xi = x/c$
ρ = air density
ϕ = azimuth, $\phi = 0$ for windward meridian
χ_ℓ = hypersonic scaling parameter, $\chi_\ell = 2\,C_{DN}^{1/2}\,(d_N/d_B)/\theta_c$
$\omega, \bar{\omega}$ = angular frequency, $\bar{\omega} = \omega c/U_\infty$

Subscripts

B,N = base and nose, respectively
cg = center of gravity or oscillation center
e = boundary-layer edge
s = surface
tr = boundary-layer transition
V = vortex
1,2 = forebody and aftbody lumped load stations, respectively (Fig. 5)
∞ = freestream conditions

Superscripts

i = transition-induced, e.g., $\Delta^i C_{m\alpha}$ = change in $C_{m\alpha}$ due to transition
$\bar{(\ )}$ = integrated mean value

Derivative Symbols

$\dot{\alpha}$ = $\partial\alpha/\partial t$
$C_{m\alpha}$ = $\partial C_m/\partial\alpha$
C_{mq} = $\partial C_m/\partial(cq/U_\infty)$
$C_{m\dot{\alpha}}$ = $\partial C_m/\partial(c\dot{\alpha}/U_\infty)$

Introduction

IT is by now well established that when boundary-layer transition moves forward of the base of a slender re-entry body, the effects on vehicle dynamics can be large. As a consequence, dynamic tests have been performed in ground facilities to provide an understanding of how transition affects the unsteady aerodynamics of a slender conical re-entry vehicle. With few exceptions, these test have been performed for one degree-of-freedom oscillations in pitch or yaw. When the lee-side flow dominates the aerodynamics, such in-plane measurements of pitch or yaw damping do provide the desired information. However, one should be cognizant of the windward-side flow effects on the out-of-plane aerodynamics.[1]

In the analytic method developed earlier for prediction of transition-induced effects on slender cone damping,[2,3] it was assumed that the transition mechanism remained unchanged for perturbations around zero angle of attack. It has since been shown that at angle of attack, transition no longer occurs through Tollmien-Schlichting instability of the axial flow but rather through inflexional instability of the crossflow. In the present paper, the original analysis[2,3] is modified to account for this fact. Unless stated otherwise, the boundary-layer transition effects discussed all concern aftbody transition; i.e., the mean position of the transition line is located aft of the oscillation center or c.g. of the vehicle. The discussion is also limited to the hypersonic and high supersonic speed ranges.

Transition Effects

On a nonablating vehicle, the boundary-layer transition has a favorable effect on the dynamic stability in pitch, as has been shown by Ward for a 10-deg pointed cone[4] (Fig. 1). The reason for this is that boundary-layer crossflow causes a forward transition movement on the leeward side, generating a negative normal force on the aftbody[4] (Fig. 2). The corresponding effect on the static stability is destabilizing. However, because of crossflow time lag effects, the corresponding effect on the dynamic stability is stabilizing,[2,3] in agreement with the experimental results[4] in Fig. 1.

Received Dec. 15, 1986; presented as Paper 87-0493 at the AIAA 25th Aerospace Sciences Meeting, Reno, NV, Jan. 12-15, 1987; revision received May 21, 1987.

*Senior Consulting Engineer. Fellow AIAA.

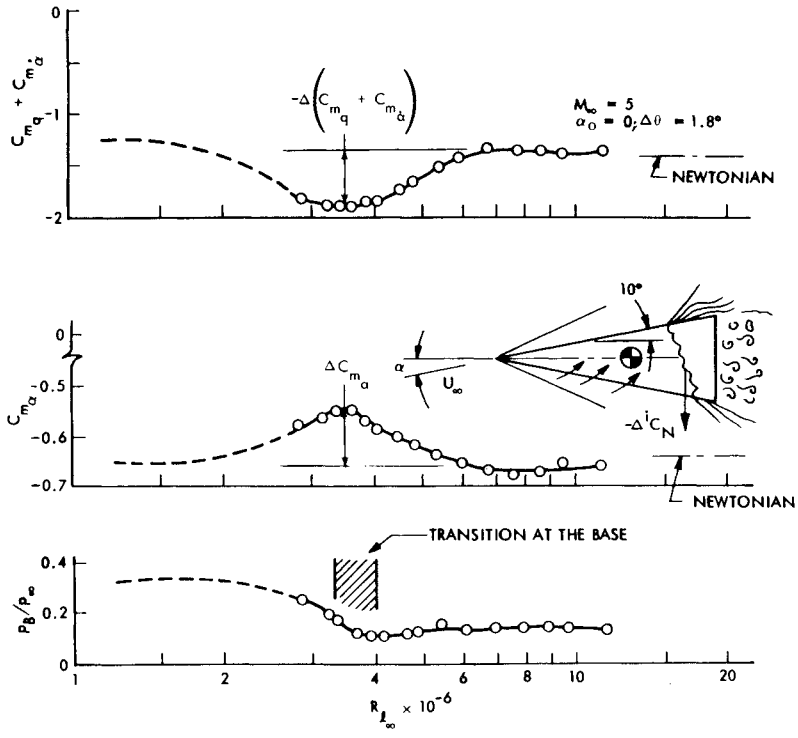

Fig. 1 Boundary-layer transition effects on sharp cone stability at $M_\infty = 5$.[4]

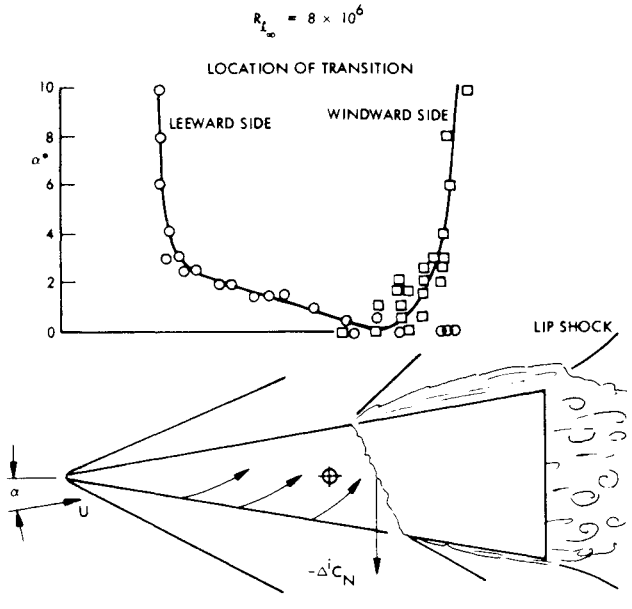

Fig. 2 Effect of angle of attack on boundary-layer transition on a 10-deg sharp cone at $M_\infty = 5$.[4]

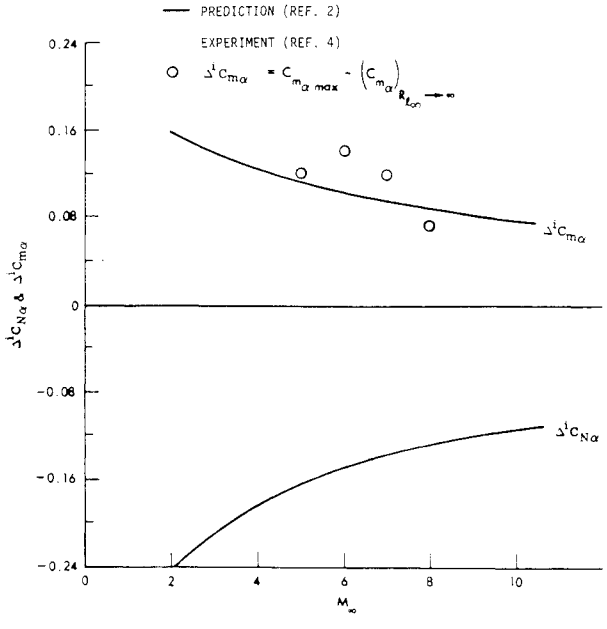

Fig. 3 Computed and measured aerodynamic effects of boundary-layer transition on a 10-deg sharp cone.

It is shown in Ref. 2 that, if the transition is represented by a straight line (see Fig. 2), the difference in displacement surface slopes for laminar and turbulent boundary layers produces a negative normal force that gives a statically destabilizing moment contribution in good agreement with the one measured experimentally[4] (Fig. 3). For the 1.8-deg oscillation amplitude used in the dynamic test, the main transition-induced effect comes from the leeward side[3] (Fig. 4), as can be expected from the experimental results[4] shown in Fig. 2. When the mean transition location moves forward of the oscillation center, $x_{cg}/\ell = 0.55$, the transition-induced effect changes sign.[3] It can be seen that, for the amplitude $\Delta\theta/\theta_c = 0.18$, the maximum transition-induced mapping occurs when transition at $\alpha = 0$ would occur half a body length aft of the base. That is, only leeward-side effects are present.

Analysis

In the original analysis,[2,3] the convective time lag effects were computed as in the case of two-dimensional and axisymmetric flow.[5,6] Forces C_{N1} and C_{N2} in Fig. 5 are of attached flow type (inviscid), whereas $\Delta^i C_N$ is the negative (aft) body force induced by differential (top and bottom) boundary-layer transition. The earlier transition on the leeward side is the result of the forebody crossflow, thickening and weakening the leeward-side boundary layer. Using the lumped force representation shown in Fig. 5, the quasisteady boundary-layer thickness can be expressed as follows:

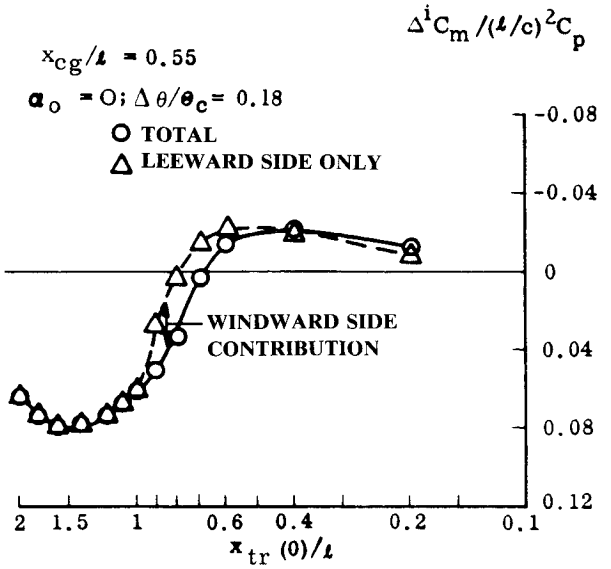

Fig. 4 Transition-induced pitching moment on a 10-deg sharp cone.[3]

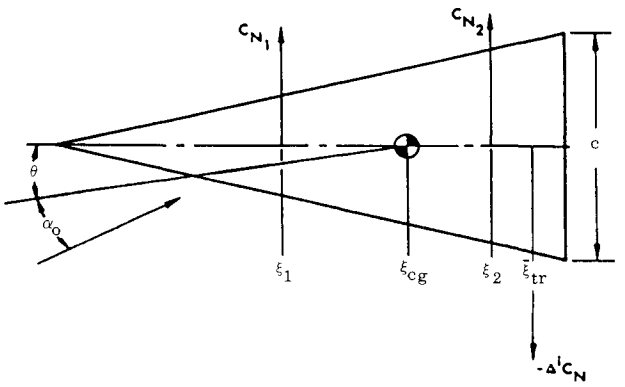

Fig. 5 Definitions for lumped force analysis.[2]

$$\delta(x_{tr},t) = (\delta)_{\substack{\alpha=0\\ \dot\alpha=0}} + (\partial\delta/\partial\alpha)_1 \tilde\alpha(x_1, t-\Delta t_1) + (\partial\delta/\partial\alpha)_2 \tilde\alpha(x_2, t-\Delta t_2) \quad (1)$$

$\tilde\alpha$ is the angular representation of body crossflow; Δt_1 and Δt_2 are the time increments occurring before changes of body crossflow at x_1 and x_2, respectively, have resulted in changed boundary-layer thickness at transition (x_{tr}). For rigid body oscillations around the center of gravity (Fig. 5), $\tilde\alpha$ is simply

$$\tilde\alpha = \alpha_0 + \theta + (\xi - \xi_{cg})c\dot\theta/U_\infty \quad (2)$$

For slow oscillations at the low reduced frequencies realizable for re-entry bodies, $\bar\omega^2 \ll 1$, $\alpha(t-\Delta t)$ can be expressed as follows:

$$\alpha(t-\Delta t) = \alpha(t) - \Delta t\dot\alpha(t) \quad (3)$$

$$\Delta t = (\bar x_{tr} - x)/\bar U = (\bar\xi_{tr} - \xi)(\bar U/U_\infty)^{-1} c/U_\infty \quad (4)$$

$\bar U$ is boundary-layer convection speed, $0.8 \le \bar U/U_\infty \le 1.0$.

Thus, the induced force $\Delta^i C_N$ at x_{tr} can be written as follows:

$$\Delta^i C_N = \Delta^i C_N(\alpha_o) + \frac{\partial\Delta^i C_N}{\partial\delta}\left(\frac{\partial\delta}{\partial\alpha}\right)_i \times \left\{\theta + \left[(\xi_1 - \xi_{cg}) - \frac{(\bar\xi_{tr} - \xi_1)}{\bar U/U_\infty}\right]\frac{c\dot\theta}{U_\infty}\right\} + \frac{\partial\Delta^i C_N}{\partial\delta}\left(\frac{\partial\delta}{\partial\alpha}\right)_2 \times \left\{\theta + \left[(\xi_2 - \xi_{cg}) - \frac{(\bar\xi_{tr} - \xi_2)}{\bar U/U_\infty}\right]\frac{c\dot\theta}{U_\infty}\right\} \quad (5)$$

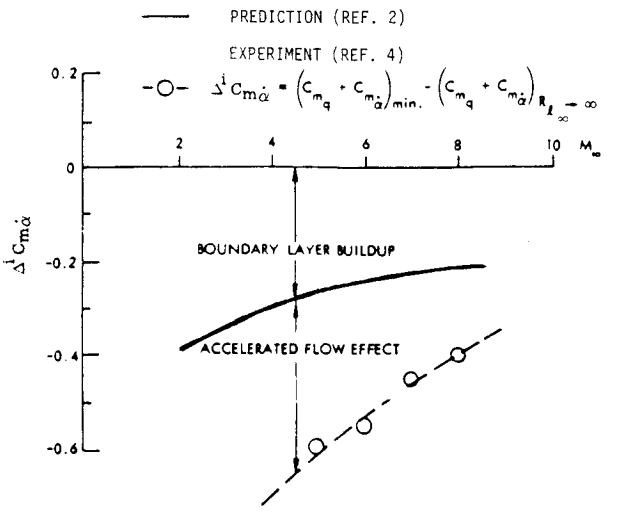

Fig. 6 Comparison between predicted and measured transition effects on sharp cone dynamic stability.[2]

If the effect of the aft body crossflow at x_2 is neglected (the effect should be small at near-zero angle of attack), Eq. (5) gives

$$\partial\Delta^i C_N/\partial\theta = (\partial\Delta^i C_N/\partial\delta)(\partial\delta/\partial\alpha)_1 = \Delta^i C_{N_\alpha}$$

$$\frac{\partial\Delta^i C_N}{\partial(c\dot\theta/\bar U_\infty)} = \Delta^i C_{N_\alpha}\left[(\xi_1 - \xi_{cg}) - \frac{(\bar\xi_{tr} - \xi_1)}{\bar U/U_\infty}\right] = \Delta^i C_{N_{\dot\alpha}} \quad (6)$$

With $\Delta^i C_m = -(\bar\xi_{tr} - \xi_{cg})\Delta^i C_N$, Eq. (6) gives the result shown in Fig. 6. It can be seen that the boundary-layer buildup effect computed in this manner does not account for the observed dynamic effect of transition.[4] The dynamic amplification of the static boundary-layer transition effect, given by Eq. (6), is

$$\frac{\Delta^i(C_{mq} + C_{m_{\dot\alpha}})}{\Delta^i C_{m_\alpha}} = \frac{\Delta^i C_{N_{\dot\alpha}}}{\Delta^i C_{N_\alpha}} = \left[(\xi_1 - \xi_{cg}) - \frac{(\bar\xi_{tr} - \xi_1)}{\bar U/U_\infty}\right] \quad (7)$$

Figure 6 shows that this boundary-layer buildup effect accounts for only part of the amplification observed on the sharp cone.[4] In the original analysis,[2,3] it was suggested that the remainder was caused by accelerated flow effects. That is, the location x_{tr} of the boundary-layer transition is not only determined by the boundary-layer buildup effect but is also dependent on the local pressure gradient and Mach number, as affected by the oscillatory perturbations. Because such accelerated flow effects have been shown to be large in the case of flow separation on slender bodies,[7] they could be expected to be large also in the case of boundary-layer transition.[2,3]

While the accelerated flow effects can be expected to be of significant magnitude at lower Mach numbers, they decline in importance with increasing supersonic Mach number and should be rather insignificant at hypersonic speeds, something that has been pointed out to me by Mark Morkovin. Consequently, the difference between prediction and experiment in Fig. 6 must have another reason. It has since been shown that, at angle of attack, the Tollmien-Schlichting type of instability mechanism is bypassed and that boundary-layer transition on the cone occurs through instability in the α-induced crossflow

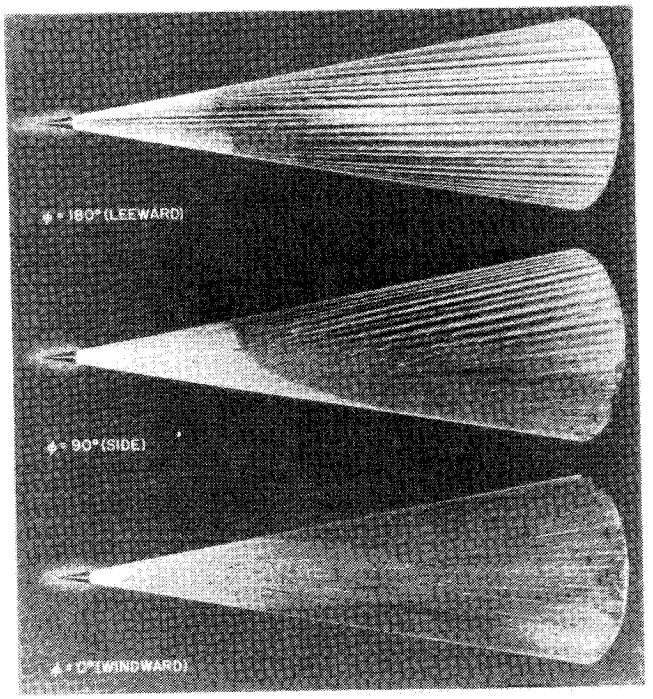

Fig. 7 Oil flow study of a 10-deg sharp cone at $\alpha = 5$ deg and $M_\infty = 7.4$.[10]

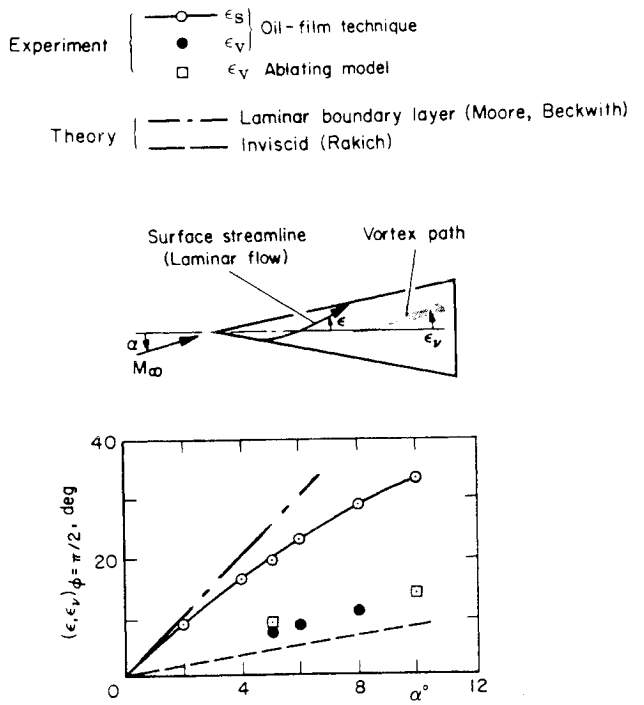

Fig. 8 Viscous flow streamline inclination at the lateral meridian.[10]

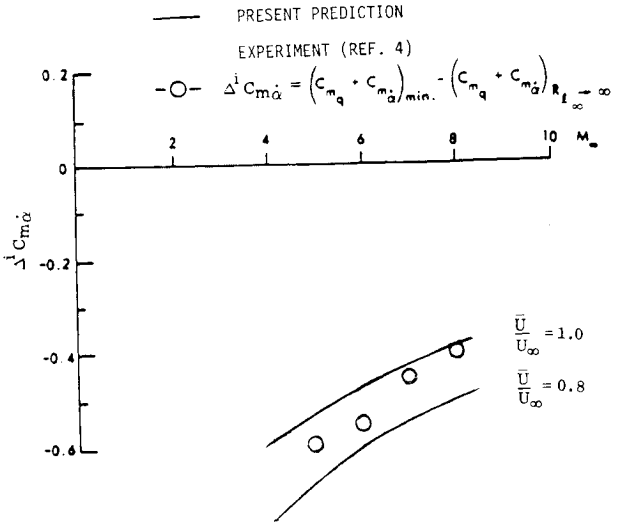

Fig. 9 Comparison between predicted and measured effect of transition on the pitch damping of a 10-deg sharp cone.

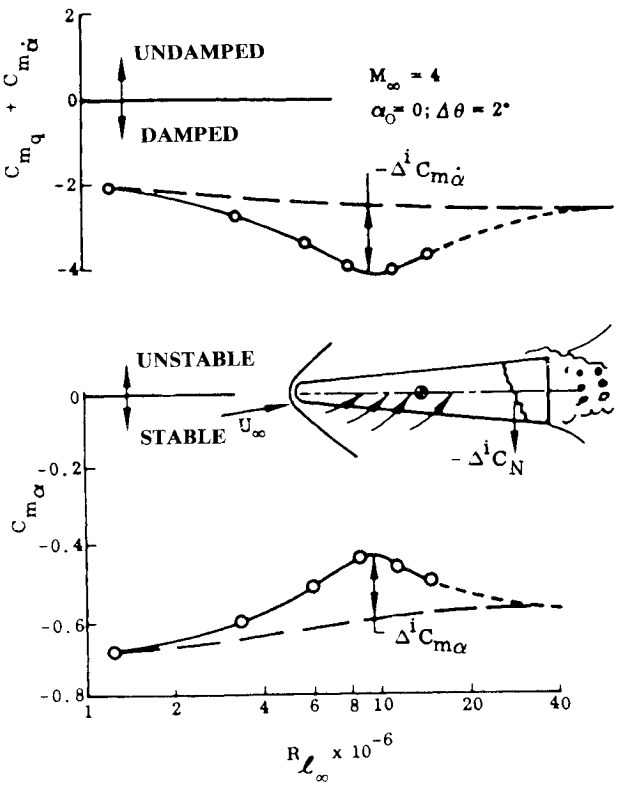

Fig. 10 Transition effects on blunted cone stability.[2]

in the presence of crossflow-induced corotating boundary-layer vortices[9,10] (Fig. 7). Thus, the convective time lagmechanism is more like that for the leading-edge vortex on a delta wing.[11]

There is still one difference, however. In the case of the sharp-edged delta wing,[11] the leading-edge vortex is fed by local crossflow from the apex to the trailing edge. This is not the case for the boundary-layer vortices. Figure 7 shows that aftbody crossflow cannot affect the top side vortices, as the vortices almost follow the inviscid streamlines[10] (Fig. 8). Thus, the boundary-layer vortices behave more like the strake vortex on a double-delta planform wing. It was found that for the double-delta wing-body configuration of the Space Shuttle Orbiter,[12] the unsteady vortex-induced effects were simulated by lumping the crossflow effects to the strake apex. In the present case, that would correspond to lumping the crossflow effects to the cone apex. This gives the following expression for the maximum transition effect:

$$\Delta^i C_{m_{\dot{\alpha}}} = -\Delta^i C_{m_\alpha} (\xi_{tr} U_\infty / \bar{U} + \xi_{cg}) \tag{8}$$

Using the computed maximum $\Delta^i C_{m\alpha}$ shown in Fig. 3, the

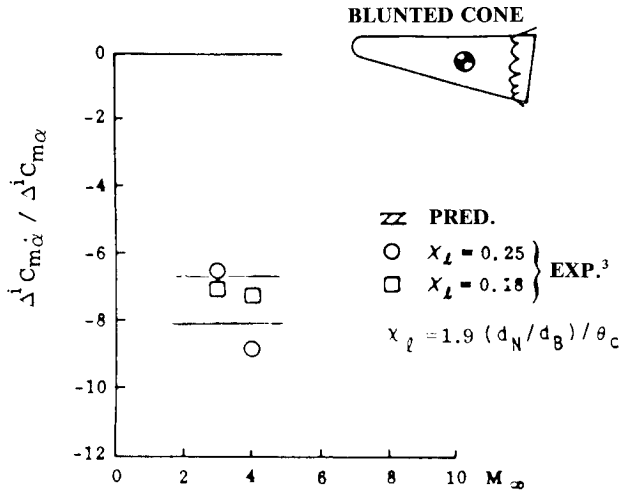

Fig. 11 Comparison between predicted and measured transition effects on blunted cone pitch damping.

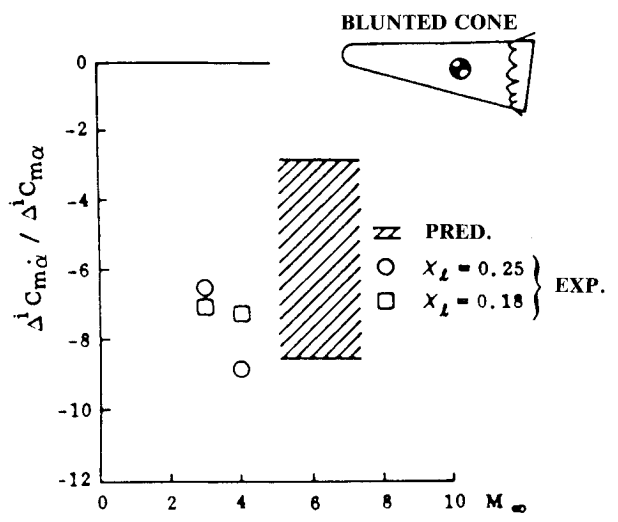

Fig. 12 Earlier comparison between predicted and measured transition effects on blunted cone pitch damping.[3]

results in Fig. 9 are obtained, showing that the experimental dynamic results are predicted much better than before[2,3] (Fig. 6). The convective velocity ratio $0.8 \le \bar{U}/U'_\infty \le 1.0$ is the same as was used earlier.[2,3]

For a slender blunted cone, Eq. (8) takes the following form:

$$\Delta^i C_{m_{\dot{\alpha}}} = -\Delta^i C_{m_\alpha} (\xi_{tr} U_\infty / \bar{U} + \xi_{cg}) / (U_e/U_\infty) \qquad (9)$$

where U_e/U_∞ is defined by embedded Newtonian theory[13] as

$$U_e/U_\infty = 0.68 + 0.42\,\chi^{1/2} \qquad (10)$$

For the experimental data illustrated in Fig. 10, one obtains the results shown in Fig. 11. It can be seen that the new prediction represents a substantial improvement over the earlier one[3] (Fig. 12). At $M_\infty \le 4$, the nose bluntness effect on the aftbody flowfield is small,[14] as is the associated entropy gradient effect on transition.[15]

As it has been shown that the lee-side flow effects, which are dominant for planar motion, are relatively insensitive to nose bluntness[16] and out-of-plane motion effects,[1] the present paper, in combination with Refs. 2 and 3, will provide a valuable tool for preliminary design.

Conclusions

Updating a previously developed analytic method to account for the fact that, at nonzero angle of attack, slender cone transition occurs through crossflow inflexional instability rather than through Tollmien-Schlichting instability of the axial flow provides predictions of transition-induced effects on pitch damping in good agreement with experimental results for sharp and blunted slender cones.

References

[1]Ericsson, L.E., "Coupling Between Vehicle Motion and Slender Cone Transition," AIAA Paper 86-1823, June 1986.

[2]Ericsson, L.E., "Effects of Boundary Layer Transition on Vehicle Dynamics," *Journal of Spacecraft and Rockets,* Vol. 6, Dec. 1969, pp. 1404–1409.

[3]Ericsson, L.E., "Transition Effects on Slender Vehicle Stability and Trim Characteristics," *Journal of Spacecraft and Rockets,* Vol. 11, Jan. 1974, pp. 3–11.

[4]Ward, L.K., "Influence of Boundary-Layer Transition on Dynamic Stability at Hypersonic Speeds," *Transactions of the Second Technical Workshop on Dynamic Stability Testing,* Paper 9, Vol. 11, Arnold Engineering Development Center, Arnold Air Force Station, TN, April 1965.

[5]Ericsson, L.E. and Reding, J.P., "Unsteady Airfoil Stall, Review and Extension," *Journal of Aircraft,* Vol. 8, Aug. 1971, pp. 609–616.

[6]Ericsson, L.E. and Reding, J.P., "Analysis of Flow Separation Effects on the Dynamics of a Large Space Booster," *Journal of Spacecraft and Rockets,* Vol. 2, July–Aug. 1965, pp. 481–490.

[7]Ericsson, L.E., "Aeroelastic Instability Caused by Slender Payloads," *Journal of Spacecraft and Rockets,* Vol. 4, Jan. 1967, pp. 65–73.

[8]Schlichting, H., *Boundary Layer Theory,* 4th ed., McGraw-Hill, New York, 1960.

[9]Pate, S.R. and Adams, J.C., "Hypersonic Simulation for Lifting Body Transition Studies," Paper 6, Vol. III, *Proceedings of the Boundary Layer Transition Workshop,* Nov. 1971, Aerospace Rept. TOR-0172, (S2816-16) 15, Oct. 1971.

[10]McDevitt, J.B. and Mellenthin, J.A., "Upwash Patterns on Ablating and Nonablating Cones at Hypersonic Speeds," NASA TN D-5346, July 1969.

[11]Ericsson, L.E. and Reding, J.P., "Unsteady Aerodynamics of Slender Delta Wings at Large Angles of Attack," *Journal of Aircraft,* Vol. 2, Sept. 1975, pp. 721–729.

[12]Reding, J.P. and Ericsson, L.E., "Effects of Flow Separation on Shuttle Longitudinal Dynamics and Aeroelastic Stability," *Journal of Spacecraft and Rockets,* Vol. 14, Dec. 1977, pp. 711–718.

[13]Ericsson, L.E., "Unsteady Embedded Newtonian Flow," *Astronautica Acta,* Vol. 18, Nov. 1973, pp. 309–330.

[14]Ericsson, L.E., "Generalized Unsteady Embedded Newtonian Flow," *Journal of Spacecraft and Rockets,* Vol. 12, Dec. 1975, pp. 718–726.

[15]Ericsson, L.E., "Entropy Gradient Effects on Blunted Cone Transition," AIAA Paper 75-195, 1975.

[16]Ericsson, L.E., "Correlation of Attitude Effects on Slender Vehicle Transition," *AIAA Journal,* Vol. 12, April 1974, pp. 523–529.